



Structural, Mechanical and Erosion Properties of Yttrium Oxide Coatings by Axial Suspension Plasma Spraying for Electronics Applications

Junya Kitamura, Zhaolin Tang, Hiroaki Mizuno, Kazuto Sato, and Alan Burgess

(Submitted May 12, 2010; in revised form September 25, 2010)

Yttrium oxide (Y_2O_3) coatings have been prepared by axial suspension plasma spraying with fine powders. It is clarified that the coatings have high hardness, low porosity, high erosion resistance against CF_4 -containing plasma and retention of smooth eroded surface. This suggests that the axial suspension plasma spraying of Y_2O_3 is applicable to fabricating equipment for electronic devices, such as dry etching. Surface morphologies of the slurry coatings with splats are similar to conventional plasma-sprayed Y_2O_3 coatings, identified from microstructural analysis. Dense coating structures with no lamellar boundaries have been seen, which is apparently different from the conventional coatings. It has also been found that crystal structure of the suspension coatings mainly composed of metastable monoclinic phase, whereas the powders and the conventional plasma spray coatings have stable cubic phase. Mechanism of coating formation by plasma spraying with fine powder slurries is discussed based on the results.

Keywords nanostructured coatings, plasma erosion, PS microstructures, suspension plasma spray, yttrium oxide

1. Introduction

The size of semiconductor and flat-panel-display (FPD) production equipment used for dry etching, sputtering, and ashing have been increasing because of the increased size of Si wafer (from 200 to 300 mm in diameter) and the FPD, where plasma treatment is effectively used for micro fabrication especially in dry etching (Ref 1). Applied power for generating plasma required to fabricate the Si and LCD devices uniformly onto the large-scaled

substrates and to achieve high etching productivity for cost reduction has also been increasing. This trend strongly promotes application of plasma-sprayed coatings by high-purity ceramics for anti-plasma erosion at inside wall of the chamber and for high electric strength (high breakdown voltage) of electrostatic chuck (ESC) as a replacement of current conventional techniques, such as anodized aluminum (alumite film) and sintered bulk ceramics (Ref 2-4). For example, inner diameter of the chamber wall is increasing from 400 to 500-600 mm in the Si device production equipment because of the enlargement of the wafer size.

It has been increasingly difficult to use the alumite film as a shield or an ESC to protect gradually the chamber parts because the halogen-contained plasma with high power erodes the film with high rate. This intense erosion generates a large amount of particles and results in frequent maintenance of the production equipment and decrease in the yield ratio of the devices due to deposition of the particles (Ref 3). The use of sintered bulk ceramics as the shielding agents also been made difficult because of the enlarged size of the equipment, and technical difficulty as well as higher cost involved in the production of large-scaled ceramics.

Plasma-sprayed ceramic coatings have technical and commercial advantages to overcome these problems, such as no limitation of the equipment size, relatively higher anti-plasma erosion resistance, higher breakdown voltage, and relatively lower cost to achieve thick coating of about a few hundred micrometers. As ceramic materials for plasma spraying, aluminum oxide (alumina, Al_2O_3) and yttrium oxide (yttria, Y_2O_3) have been utilized until now

This article is an invited paper selected from presentations at the 2010 International Thermal Spray Conference and has been expanded from the original presentation. It is simultaneously published in *Thermal Spray: Global Solutions for Future Applications, Proceedings of the 2010 International Thermal Spray Conference*, Singapore, May 3-5, 2010, Basil R. Marple, Arvind Agarwal, Margaret M. Hyland, Yuk-Chiu Lau, Chang-Jiu Li, Rogerio S. Lima, and Ghislain Montavon, Ed., ASM International, Materials Park, OH, 2011.

Junya Kitamura, Hiroaki Mizuno, and Kazuto Sato, Thermal Spray Materials Department, Fujimi Incorporated, Kakamigahara, Gifu, Japan; and Zhaolin Tang and Alan Burgess, Northwest Mettech Corporation, 467 Mountain Highway, North Vancouver, BC, Canada. Contact e-mail: kitamuraj@fujimiinc.co.jp.



because of their high durability against the halogen-contained plasma (Ref 3-5). In particular, spraying technique seems to be better for Y_2O_3 because of its high brittleness and high cost.

Recent systematic studies by Kitamura et al. have revealed that plasma-sprayed Y_2O_3 coatings have higher plasma erosion resistance than Al_2O_3 coatings as well as sintered bulk Al_2O_3 against CF_4 -containing plasma at the actual conditions in semiconductor fabrication processes (Ref 6-8). The studies have also found that sintered bulk Y_2O_3 is still superior to plasma-sprayed coatings in terms of the plasma erosion resistance and retention of smoother eroded surface. Although the previous studies have clarified that the use of agglomerated-and-sintered Y_2O_3 powder consisting of large primary particles of about $5\ \mu m$ is effective for producing high anti-plasma erosion resistance retaining smooth surface, which may help prevent generation of large-sized particles, the surface roughness is still higher than that of the bulk (Ref 7, 8). The inferiority of the Y_2O_3 coating of erosion resistance with roughness of the eroded surface has shown that further improvement is still required for plasma spray coating.

Dense Y_2O_3 coatings are considered to be one of the solutions to improve these properties, such as plasma erosion resistance and smooth eroded surface. Using finer powders less than $10\ \mu m$ has been found to be effective to prepare denser coatings with thinner lamellae splats compared to traditionally sized powders (Ref 9, 10). Suspension plasma spraying, which process was invented in the mid-1990s by The University of Sherbrooke in Canada (Ref 11, 12), is capable to deliver the fine powders into the plasma plume, which result in formation of dense coatings, preferred porous coatings, and preferred fine structure (Ref 13, 14). In this process, several studies have been conducted by feeding nano- or micropowders as well as solution precursors to several plasma torch, such as radio-frequency (RF) (Ref 15-17) and direct-current (DC) (Ref 18-21). Injection systems, which are important key factors in the suspension plasma spraying, have also been studied using mechanical injection (Ref 13, 18, 19) and spray atomization (Ref 13, 22-25). The atomization is extensively used.

Furthermore, direction of injection, whether radial or axial, is also an important parameter, where radial and axial injections are applied to DC and RF, in general. Axial IIITM (Northwest Mettech Corp., North Vancouver, BC, Canada) system is capable of combining DC plasma and axial feeding of suspension (Ref 26-28). By suspending the fine powders in liquid and injecting the suspension axially into the plasma plume using the system, particle velocity has reached $600\ m/s$ (Ref 29) demonstrating that dense coating structures can be obtained (Ref 29, 30).

In this article, Y_2O_3 coatings have been prepared with high power axial injection plasma spraying using fine powder slurries to make dense coating structure (Ref 31). Erosion properties have been investigated against CF_4 -containing plasma by comparing among the coatings: (i) high power suspension plasma spray coatings, (ii) high power plasma spray coatings using fine powder, (iii) high power plasma spray coatings using powder of conventional

size (i.e., a few ten microns), and (iv) conventional plasma spray coating using powder of the conventional size. Basic coating properties, such as microstructure including porosity, crystal structure, and hardness have been studied among the coatings to understand the mechanism that affect the plasma erosion properties.

2. Experimental Procedure

2.1 Spray Powders and Slurries

Three types of Y_2O_3 powders, agglomerated, sintered, and conventional, manufactured by Fujimi Inc. (Kakamigahara, Gifu, Japan) were used in this study: DTS-Y27-63/10 (Y-c; $d_{50} \sim 37\ \mu m$); DTS-Y34 (Y-f5, $d_{50} \sim 5\ \mu m$); and DTS-Y35 (Y-f1, $d_{50} \sim 1\ \mu m$), respectively. SEM micrographs of the powders are shown in Fig. 1. Average powder diameters of d_{50} were estimated using laser diffraction and scattering method (LA-300, Horiba Co. Ltd., Kyoto, Japan). The conventional sized powders (Y-c) and Y-f5 were fed to plasma torch by conventional method. Suspension feeding was carried out for the other two fine powders. Based on the suspension optimization, the suspension solid concentration was set at 10 wt.% in ethanol based solvent. Sintered bulk Y_2O_3 materials (Y-bulk, $15 \times 15 \times 2\ mm$), which were manufactured by Fujimi Inc., were used as a reference material.

2.2 Preparation of Plasma Spray Coatings

Table 1 summarizes specimens prepared in this study with feedstock powders, under plasma spray conditions. Atmospheric plasma spraying using SG-100 (Praxair, Cincinnati, OH, USA) with Y-c was used to prepare a conventional coating (c-SG). The plasma power was 32 kW, and other spray conditions employed are summarized in Table 2. The powders were fed along radial direction into plasma plume in this plasma spray equipment. Axial IIITM was used for producing high-power plasma spray coatings of c-Ax and f5-Ax as well as high power suspension plasma spray coatings of f5s-Ax-Ar, f1s-Ax-Ar and f1s-Ax-N. The conditions are described in Table 3 in detail where the plasma power is about 90 kW. Both powders and slurries were fed axial direction into plasma plume when using Axial IIITM. The NanofeedTM Model M650 Liquid Powder Feeder (Northwest Mettech Corp.) was used to deliver fine micron powders in a suspension form into the plasma plume. The Nanofeed 650TM is a new device that precisely feeds suspension mixtures using mass flow control of both suspension and atomizing gas to provide uniform atomization at the injector with high reliability. Thicknesses of all the coatings were adjusted ranging from 150 to 250 μm . All the spray conditions were adjusted to keep white-colored coatings. In particular, dry feeding of Y-f5 tended to easily form black-colored coating, and then plasma power (enthalpy) should be lowered. On the other hand, all suspension coatings were easily kept as white colored in spite of using similar or fine-sized powders. Schematic of spraying setup for suspension

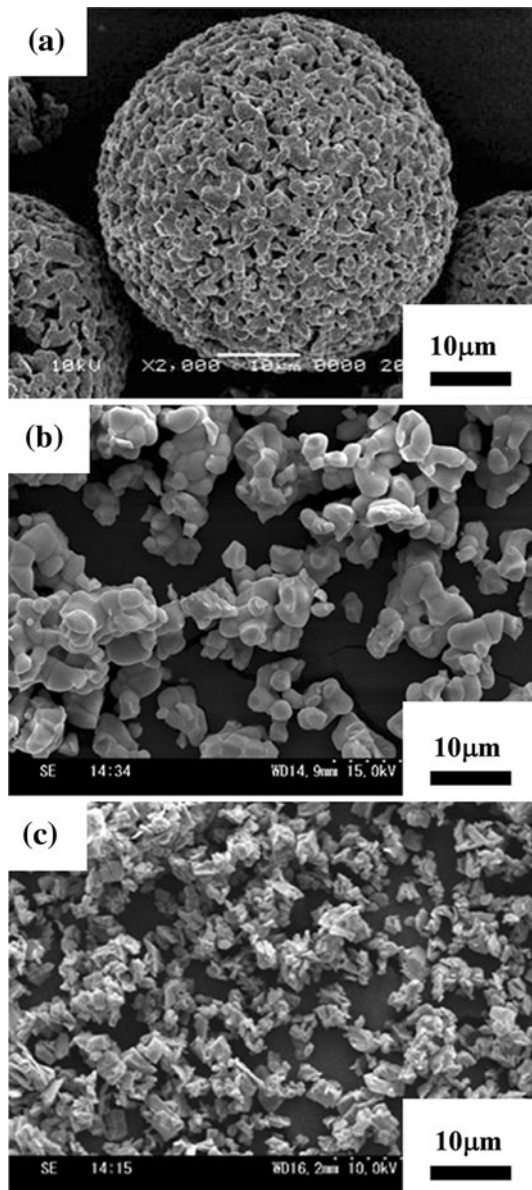


Fig. 1 SEM micrographs of Y_2O_3 powders: (a) DTS-Y27-63/10 (Y-c: $d_{50} \sim 37 \mu\text{m}$), (b) DTS-Y34 (Y-f5, $d_{50} \sim 5 \mu\text{m}$), and (c) DTS-Y35 (Y-f1, $d_{50} \sim 1 \mu\text{m}$)

Table 1 Specimens with feedstock powders and plasma spray conditions

Specimen	Powder	d_{50} , μm	Plasma gun	Powder feeding	Spray conditions
c-SG	Y-c	37	SG-100	Dry	Table 2
c-Ax			Axial III TM		Table 3(a)
f5-Ax	Y-f5	5			Table 3(b)
f5s-Ax-Ar				Suspension	Table 3(c)
f1s-Ax-Ar	Y-f1	1			Table 3(d)
f1s-Ax-N					
Y-bulk	Sintered Y_2O_3 ($15 \times 15 \times 2'$ mm)				

spraying is shown in Fig. 2 (top view), where extra care is exercised to avoid overheating the substrate due to shorter spray distance. Air cooling and fast traverse speed of

Table 2 Conditions of conventional plasma spraying (SG-100)

Parameters	Conditions
Ar/He flow rate, L/min	39/7.9
Power, kW	32
Powder feeding rate, kg/h	0.9
Spray distance, mm	120

Table 3 Conditions of high power plasma spraying (Axial IIITM)

Parameters	Conditions			
	(a)	(b)	(c)	(d)
Ar/N ₂ /H ₂ flow rate, L/min	90/54/36	75/5/20	168/23/29	81/81/18
Power, kW	96	90	83	88
Powder feeding rate, kg/h	3	1
Slurry (powder) feeding rate, kg/h	1 (0.1)	2 (0.2)
Spray distance, mm	100		50	

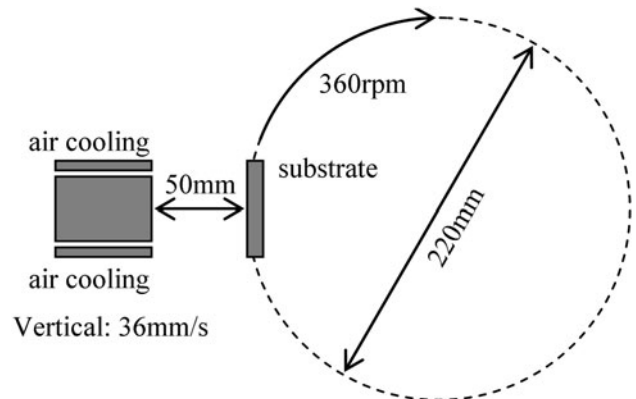


Fig. 2 Schematic of spraying setup for suspension spraying (top view)

about 4100 mm/s have been applied so that the substrate temperature at backside is kept less than 200 °C, being measured by thermocouple.

Substrates of aluminum alloy (A6061, $50 \times 70 \times 2 \text{ mm}^3$) were sand blasted by alumina grit before plasma spraying. Surfaces of sprayed coatings cut to $15 \times 15 \text{ mm}$ and sintered Y_2O_3 were mirror polished using colloidal silica polishing slurry with an average diameter of $0.06 \mu\text{m}$ to study both the durability against the CF_4 containing plasma and the erosion mechanism in detail for the plasma erosion test later described. Coating thickness after the mirror polishing was $\geq 100 \mu\text{m}$.

2.3 Evaluation of Coating Properties

Scanning electron microscopies (SEM: S3000, Hitachi High-Technologies Corp., Tokyo, Japan) and field emission SEM (FE-SEM: S4700, Hitachi High-Technologies Corp.) were carried out for microstructural analysis. Porosities of the coatings were estimated by image analysis from optical micrographs (VC7700, OMRON Corp., Kyoto, Japan). Sample of cross sections for coating were prepared by mechanical polishing using colloidal silica slurry, to yield a final average diameter of $0.06 \mu\text{m}$. Micro Vickers hardness (HMV-1, Shimadzu Corp., Kyoto, Japan) was measured with load and loading time of 1.96 N (200 gf) and 10 s , respectively. Crystal structures of the powders and the coatings were identified from x-ray diffraction analysis (XRD: ULTIMA IV, RIGAKU Corp., Akishima, Tokyo, Japan).

2.4 Evaluation of Plasma Erosion Test

Conditions of the plasma erosion tests are summarized in Table 4. Reactive ion etching (RIE) equipment (NLD-800: ULVAC, Chigasaki, Kanagawa, Japan) was used in this study, where high density plasma was generated using neutron loop discharge to etch the objects, such as Si wafer and glass for display, with high rate. Before introducing into the RIE chamber (Fig. 3a), the surface of the mirror-polished specimens was partially masked by polyimide tape outside as shown in Fig. 3(b). Then, eroded area was centered around $5 \times 5 \text{ mm}^2$. The erosion rate was estimated by measuring the step height between masked area and eroded area using stylus method (SV-3000CNC, Mitsutoyo Corp., Kawasaki, Kanagawa, Japan). Possibility to generate large-sized particle was discussed through microstructural analysis of the eroded surface by SEM and the stylus method.

Table 4 Conditions of the plasma erosion test using RIE (NLD-800, ULVAC, Japan)

Parameters	Conditions
Ar/CF ₄ /O ₂ flow rate, mL/min	95/9.5/1.0
Chamber pressure, Pa	1
Plasma power, W	400
Exposure area, mm in diameter	100
Exposure time, min	52.5
Exposure cycle, min	
Exposure	0.5
Interval	3.0

2.5 Effect of Substrate Roughness on Inhomogeneity of Suspension Coatings

Macro roughness features, sometimes called as protrusions, nodules, or speckles, appeared on suspension coating surface found through our preliminary studies (Ref 31). This inhomogeneous structure should be removed generally because coating properties would be degraded (Ref 32). In order to find formation mechanism, suspension coatings of fls-Ax-N have been formed onto smooth and rough substrate with changing coating thickness as summarized in Table 5. Rough substrate preparation was the same as that described in section 2.2. Average surface roughness (R_a) of each specimen was measured using stylus method (SV-3000CNC, Mitsutoyo Corp., Kawasaki, Kanagawa, Japan).

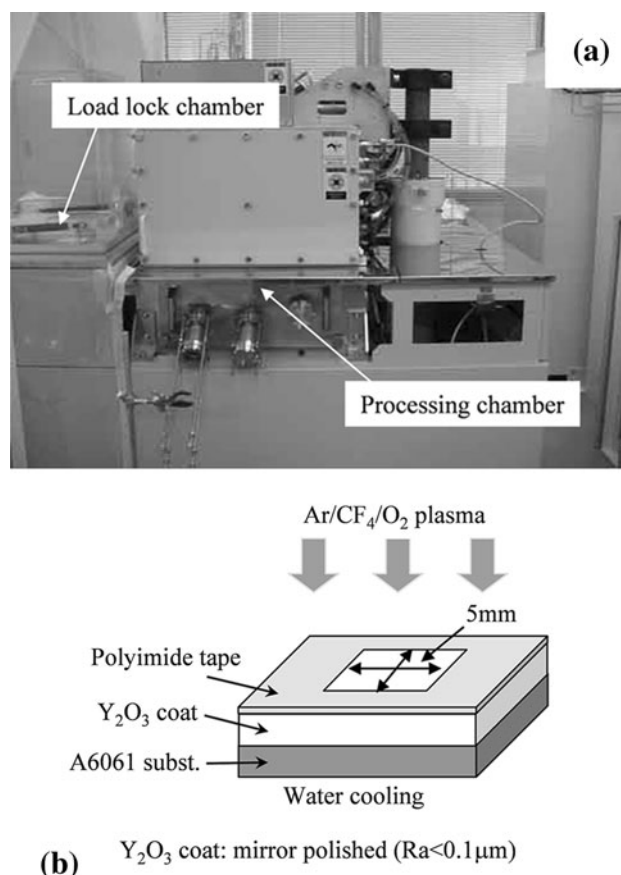


Fig. 3 (a) RIE equipment and (b) specimens prepared for plasma erosion test

Table 5 Specimens to study effect of substrate roughness on coating inhomogeneity

Substrate	Smooth	Rough
R_a , μm /Deviation of R_a , μm	0.023/0.002	1.705/0.105
Coating thickness, μm	5, 10, 20, and 50	5, 10, 20, and 50

3. Results and Discussion

3.1 Microstructure

Cross-sectional SEM micrographs of the coatings are shown in Fig. 4. The c-SG coating in Fig. 4(a) was prepared after mirror polishing of the surface, and the other coatings were prepared from as-sprayed specimens. It is clear that the suspension coatings have dense structure with a few large-sized pores normally seen in the conventional spray coatings as shown in Fig. 4(a) and (b). No distinguishable microstructural difference is seen between Fig. 4(a) and (b) in spite of using different plasma guns with different plasma powers and powder injection directions being used with the same powder (Y-c). Powder size seems to be dominant for coating microstructure based on a comparative analysis as demonstrated in Fig. 4(a)-(c).

Suspension technique with fine powder is also effective for producing denser coating. Rugged surface morphologies are observed in the suspension coatings of Fig. 4(d) and (e), whereas microstructure of the coating by dry-fed fine powder in Fig. 4(c) is different in terms of the absence of the rugged morphology and high porosity. Although its formation mechanism is unclear, atomization of suspension when injecting plasma plume may be important because a large-sized droplet lead to a large splat. Figure 4(f) shows that smoother surface are formed by adjusting suspension plasma spray conditions.

Porosity of the coatings is shown in Fig. 5, which has been estimated using image analysis of the optical micrographs of cross sections. Porosity of the suspension coatings around 0.3-0.4% is apparently lower than that of the conventional coatings (c-SG and c-Ax) by >4%, and that of the coating by dry-fed fine powder (f5-Ax) by about 3.5%.

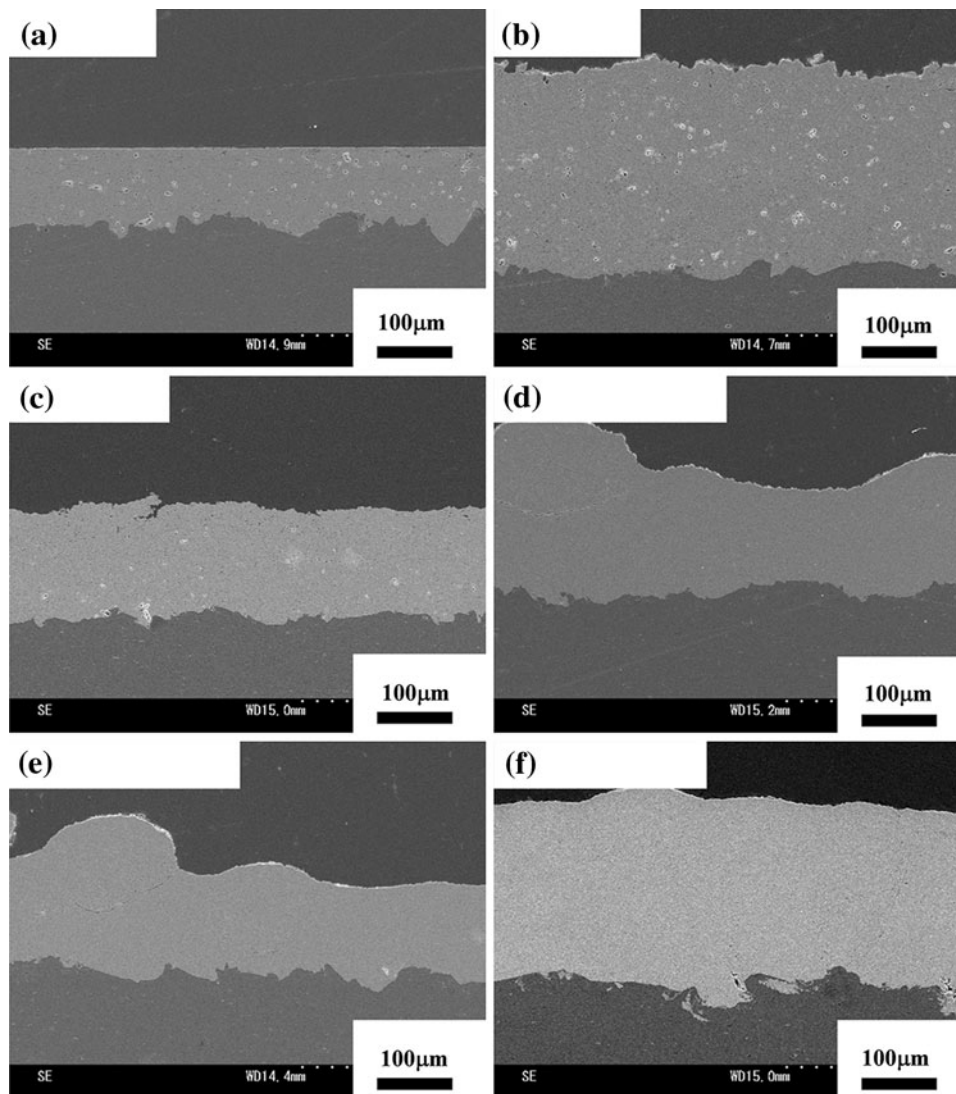


Fig. 4 Cross-sectional SEM micrographs of the coatings: (a) c-SG, (b) c-Ax, (c) f5-Ax, (d) f5s-Ax-Ar, (e) f1s-Ax-Ar, and (f) f1s-Ax-N

It is assumed that the coating with high porosity for f5-Ax is produced by inappropriate spray parameters in spite of using fine powder. Coating color was easily changed to gray or black from white color in feedstock when using dry feeding with fine powder. The spray parameters were adjusted to keep white colored coating in this study so that they might produce the porous coating because of insufficient heat and acceleration of the powder during spraying.

Microstructures of the coatings of c-SG, c-Ax, f5-Ax, and f5s-Ax-Ar are shown in Fig. 6. Magnified cross-sectional images by FE-SEM are also shown in Fig. 7 for

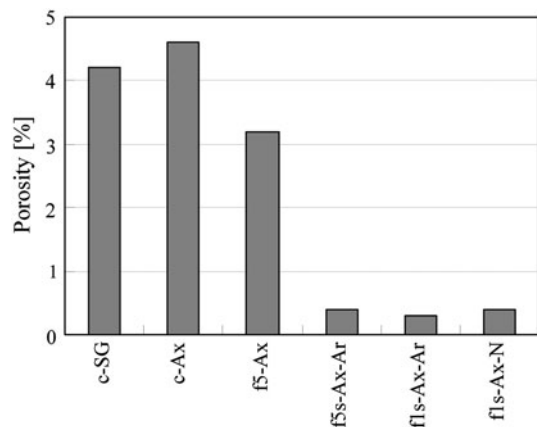


Fig. 5 Porosity of the coatings

the coatings by fine powders of f5-Ax, f5s-Ax-Ar, f1s-Ax-Ar, and f1s-Ax-N. In the c-SG coating, shown in Fig. 6(a), lamellar structure is observed, which is usually existing in the plasma spray coatings. Relatively large-sized pores of around 5-10 μm are also seen along with splat boundaries which suggest insufficient bonding among the splats. Lamellar structure is unclear and smaller-sized pores are observed in Fig. 6(b) in spite of similar porosities. It is surmised that high velocity impact of the powder by Axial III plasma gun contributes to this unclear splat boundaries.

Depositions of smaller splats and small-sized pores are observed in the f5-Ax coating prepared by dry-fed fine powder as shown in Fig. 6(c) and 7(a). Clear lamellar boundaries also suggest insufficient bonding among the splats, though fine powder is easily molten in plasma plume. Suspension coating of f5s-Ax-Ar, shown in Fig. 6(d), using same Y-f5 powder as for f5-Ax coating is apparently different and shows relatively high homogeneity without lamellar boundaries. Pore size is quite small with around micron or sub-micron scale as shown in Fig. 7(b). Coating microstructures seem to be much finer when using finer powder of Y-f1 as shown in Fig. 7(c) and (d). This suggests high bonding strength between the splats in the suspension coatings.

3.2 Surface Morphologies

Figure 8 shows SEM images of the surfaces of as-sprayed coatings with tilt angle of 30°. Surface morphologies are quite different among conventional powder

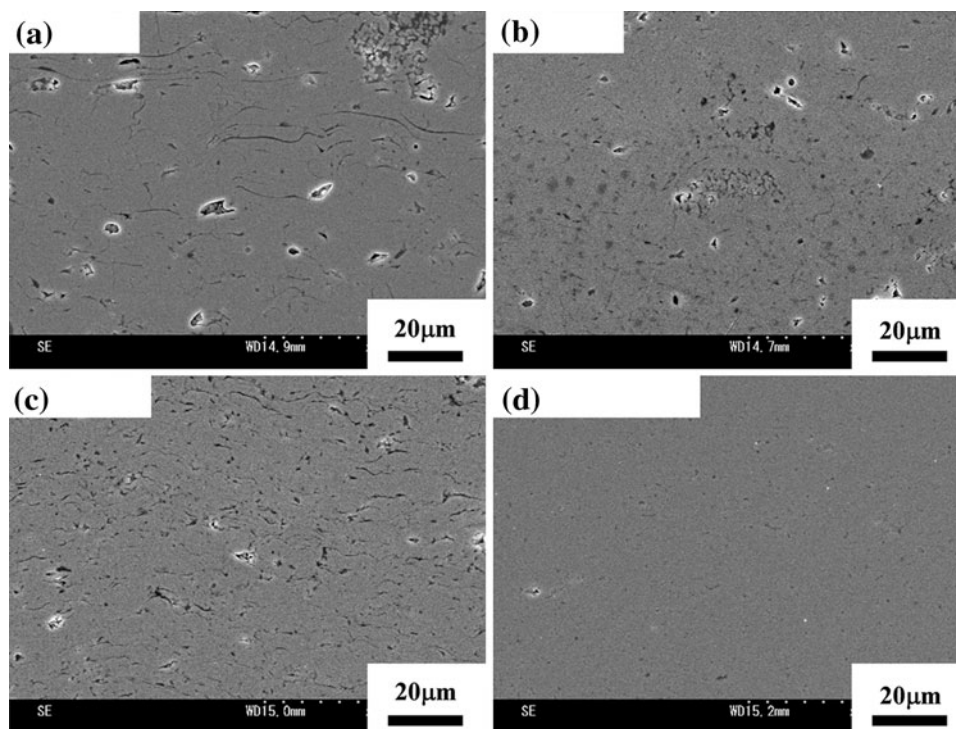


Fig. 6 Microstructures of the coatings of (a) c-SG, (b) c-Ax, (c) f5-Ax, and (d) f5s-Ax-Ar

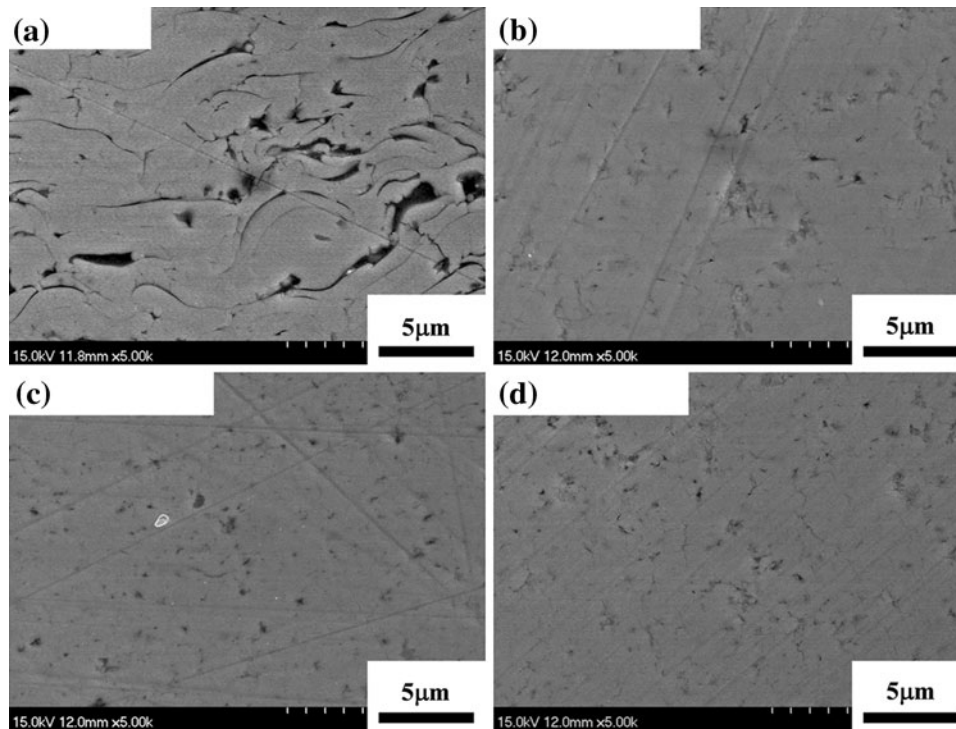


Fig. 7 Magnified cross-sectional FE-SEM images of (a) f5-Ax, (b) f5s-Ax-Ar, (c) fls-Ax-Ar, and (d) fls-Ax-N

(a, b), dry-fed fine powder, (c) and suspension (d-f). It is suggested that conventional powder of Y-c has been well molten during plasma plume by conventional plasma spraying (SG-100) from the splat morphology as shown in Fig. 8(a). As for the coating by high-power plasma spraying in Fig. 8(b), spherical-shaped deposits are observed. This implies insufficient melting of powders in the plasma plume due to short residence time by high velocity, which is obtained by high plasma velocity of up to 1000 m/s (Ref 26), 2-3 times higher than conventional plasma torch. High velocity impact of the molten powders also may cause splashing that generates such a small-sized spherical deposits.

Small-sized splats are seen in Fig. 8(c), whose morphology is reasonable by use of fine powder. This suggests that well-molten fine particles are deposited. As for the suspension coating of f5s-Ax-Ar in Fig. 8(d), surface morphology is finer with spherical-shaped deposits than that of the coating as shown in Fig. 8(c), in spite of using same powder of Y-f5. Furthermore, morphologies tend to become much finer with decreasing powder size in the suspension coatings as shown in Fig. 8(e) and (f).

Magnified FE-SEM images of the as-sprayed coating surface only for using fine powders are shown in Fig. 9 without tilt of the specimens. Pancake-shaped splats are clearly seen in the f5-Ax coating with a small amount of fine spherical deposits. Although the shape is complicated, splats are also seen in the suspension plasma coatings in Fig. 9(b)-(d). A lot of fine spherical deposits are also observed resulting in finer coating morphologies.

The sizes of both the splats and the spherical deposits are smaller when using fine powder of Y-f1 within the suspension coatings.

3.3 Vickers Hardness

Figure 10 shows Vickers hardness (HV) values of the coatings and bulk as a reference. Twelve indentation tests were performed in each specimen, and averaged HV values were obtained from ten tests by eliminating maximum and minimum values. HV values are typically ranging from 400 to 500 when using conventional plasma spray equipment and conventional-sized powders as demonstrated in our previous investigation (Ref 33). 400 HV of the c-SG coating is within the range, and the wide dispersion of the hardness shows inhomogeneous coating structure.

The result clearly shows that hard Y_2O_3 coatings of more than 600 HV have been successfully formed by high-power plasma spraying of Axial III™ except for f5-Ax. Considering that higher hardness of c-Ax than that of c-SG and similar porosities between these coatings, Axial III™ is considered to have better ability to increase bonding strength between lamellae, consistent with the microstructures. In particular, suspension coatings with fine powder of Y-f1 tend to have higher hardness around 620-640 HV. Such a high hardness is never seen in spray coatings as far as we know. However, the suspension coatings still have lower hardness than sintered bulk Y_2O_3 (700 HV) in spite of quite lower porosity. This suggests

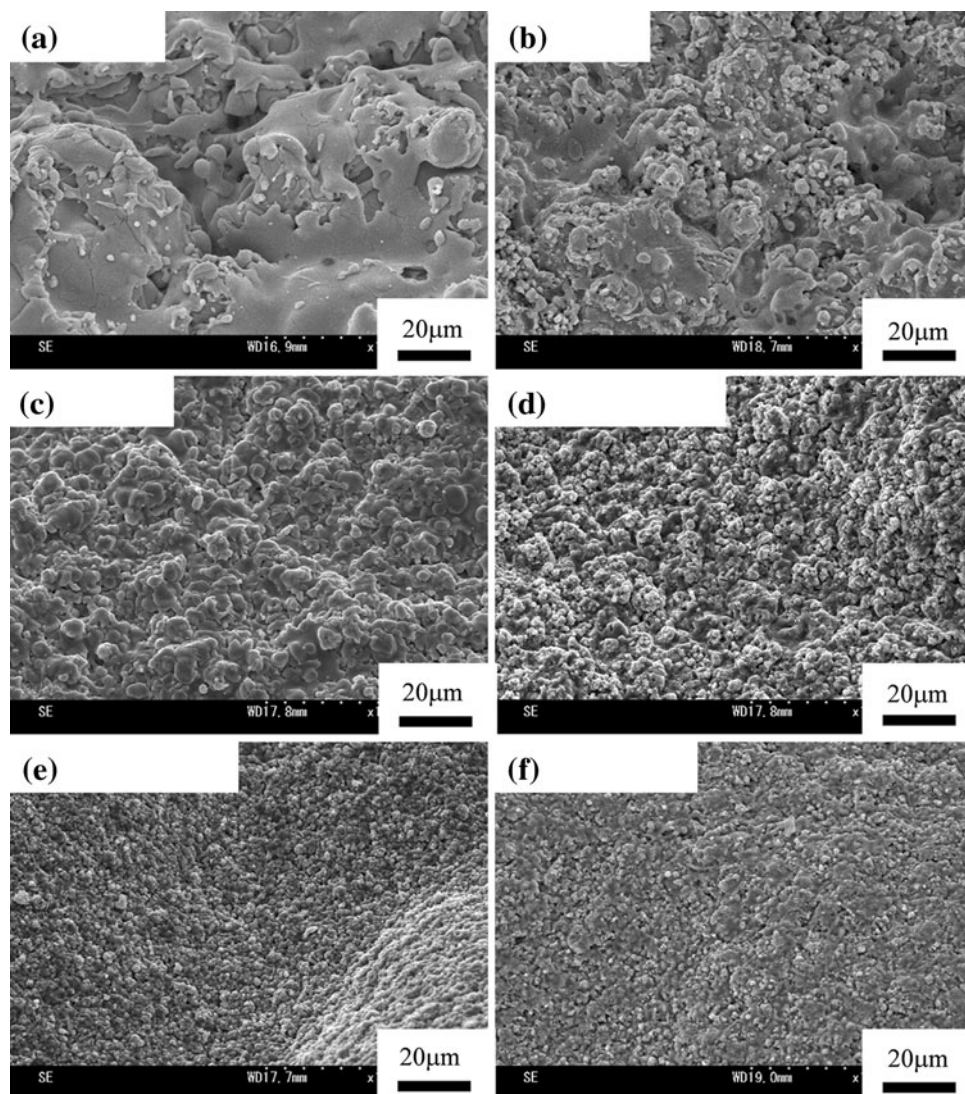


Fig. 8 SEM images of the surfaces of as-sprayed coatings: (a) c-SG, (b) c-Ax, (c) f5-Ax, (d) f5s-Ax-Ar, (e) f1s-Ax-Ar, and (f) f1s-Ax-N

that there still remains ample scope for improving the quality of suspension plasma spray coatings.

3.4 Crystal Structures

Crystal structures of the coatings have been investigated by x-ray diffraction as shown in Fig. 11. Crystal structure of all feedstock powders of Y-c, Y-f5, and Y-f1 is only composed of cubic phase, which is well known as stable phase (Ref 34). Little or no phase change has been observed for the coatings from the Y-c powder (c-SG and c-Ax). In the case of using smaller powder of Y-f5, although cubic phase is still dominant, another phase which is identified as metastable phase of monoclinic phase, has appeared in the f5-Ax coating. The peak intensities of monoclinic phase becomes higher in the suspension coatings. Comparing between the XRD patterns for f5s-Ax-Ar and f1s-Ax-Ar, the f1s-Ax-Ar

coating from smaller powder relatively contains high amount of monoclinic phase. Maximum peak of the f5s-Ax-Ar coating is still cubic phase at 29.15° $\langle 222 \rangle$. Monoclinic phase at 33.10° $\langle 11-2 \rangle$ has a maximum intensity for the f1s-Ax-Ar coating. Furthermore, cubic phase has almost changed to monoclinic phase in the f1s-Ax-N coating.

Vogt has reported formation of monoclinic phase of Y_2O_3 (Ref 35). In that report, cubic phase of yttrium oxide powder of less than $45 \mu m$ has been introduced into RF Ar-plasma (40 kW) chamber to vaporize or melt. Heated Ar gas with yttrium oxide has been quenched, and the powders have been collected using separation (size classification) system. As a result, the collected nanosized powder less than 100 nm mainly composed of monoclinic phase. Atou et al. have also reported phase transition of sintered Y_2O_3 from cubic to monoclinic due to shocked load around 20 GPa (Ref 36).

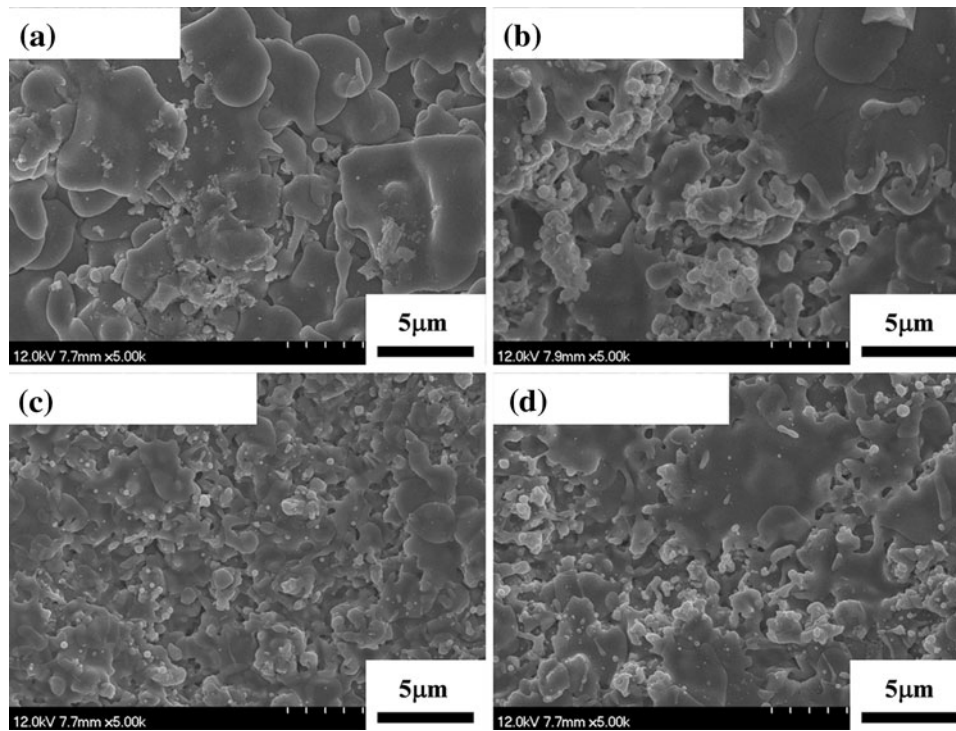


Fig. 9 Magnified FE-SEM images of the as-sprayed coating surface: (a) f5-Ax, (b) f5s-Ax-Ar, (c) fls-Ax-Ar, and (d) fls-Ax-N

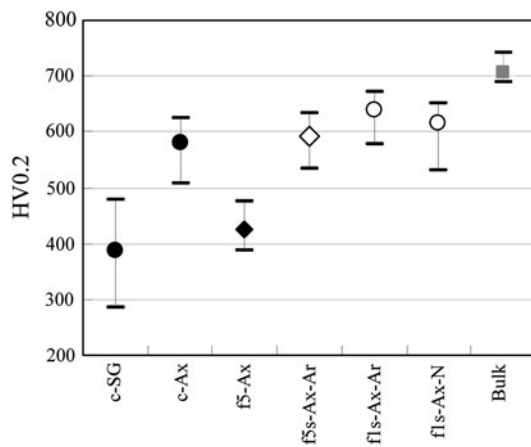


Fig. 10 Vickers hardness (HV) of the coatings and bulk

Based on the previous studies, it is considered that quenching process is necessary to make monoclinic phase of Y_2O_3 , the phenomenon of which might be similar to gamma phase formation of aluminum oxide in the plasma spraying. Use of finer powder (Y-1f) as well as of high enthalpy plasma (Nitrogen) is considered to be effective for producing powder with improved quality with increasing temperature. The highly heated powder might contribute to formation of monoclinic phase effectively through intense quenching onto the substrates.

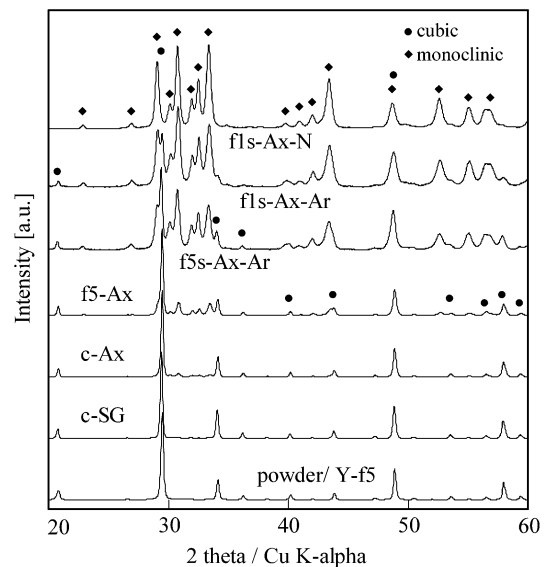


Fig. 11 X-ray diffraction patterns for powder of Y-f5 and all coatings

3.5 Plasma Erosion Resistance

Erosion rates of the Y_2O_3 coatings are shown in Fig. 12 against Ar/CF₄/O₂ plasma of 400 W, where the rate of bulk Y_2O_3 (45 nm/min) is defined as a reference. All coatings prepared by Axial III™ have higher erosion resistance than the conventional coating of c-SG and are

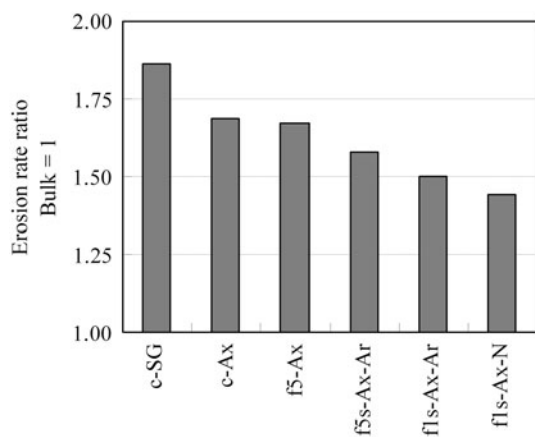


Fig. 12 Erosion rate ratio of the coatings against Ar/CF₄/O₂ plasma, bulk as a reference

inferior to the bulk. Use of fine powder with dry feeding seems to have little effect on increasing the resistance in comparison with c-Ax and f5-Ax. The suspension coatings showed higher erosion resistance than dry-fed coatings of c-SG, c-Ax, and f5-Ax. In particular, using finer powder of 1 μm (Y-f1) is more effective to obtain better properties than using 5 μm (Y-f5). Erosion rate of the best coatings of f1s-Ax-N were approximately 65 nm/min, which was <0.8 time less than that of the conventional c-SG coating (85 nm/min) and was about 1.4 times higher than that of the bulk Y₂O₃ (45 nm/min). As the c-SG coating is similar to the coatings utilized in actual production equipment, it can be considered that lifetime is extended about by 1.2-1.3 times longer when applying the suspension techniques.

Previous studies (Ref 8, 33) have reported that no improvement of the erosion resistance is confirmed when changing primary particle size of Y₂O₃ in agglomerated and sintered powders, which is almost similar to the c-SG. This suggests technical limit of conventional plasma spraying using conventional powder. Thus, it can be said that suspension feeding of fine Y₂O₃ powders, axial injection and high-power plasma spraying, which are conducted in the study, are quite effective to improve the coating properties, such as reduction in porosity (leading to improving coating uniformity) and increased hardness, as well as increased plasma erosion resistance.

3.6 Eroded Surface

Figures 13 and 14 show SEM images of the surfaces before (mirror-polished surfaces) and after (eroded surfaces) the plasma erosion test, respectively. Microstructures of polished coating surfaces are almost similar to those of cross sections as shown in Fig. 6 and 7. The suspension coatings have much smoother surfaces than the coatings by dry feeding. Large pits are observed in the sintered bulk.

It is clear that coatings prepared by conventional coarser powder (Y-c) have rougher eroded surfaces suggesting that large particles are generated and are easily

deposited onto the Si wafer. On the other hand, use of finer powders (Y-5f and Y-1f) is found to be effective to retain smoother eroded surfaces in both dry feeding and suspension feeding. This suggests generation of only smaller particles. Since the RIE keeps evacuating using vacuum pump at etching process, small particles are easily exhausted from the chamber, which is effective in terms of increased yield ratios of the Si devices due to reduction of deposition onto the device.

Surface profiles of after the plasma erosion test are shown in Fig. 15 with eroded (center) and masked (both ends) areas. The profiles are obtained by averaging from eight measured profiles using stylus method after correction of slope and curvature. In addition to high plasma erosion resistance, it is apparent that suspension coatings are quite effective to maintain smooth eroded surface. Bulk also retains smoother eroded surface except for deep pits that originally existed. Suspension coatings and bulk tend to have higher hardness than conventional coatings, suggesting a higher toughness. This might contribute to higher plasma erosion resistance.

3.7 Relation Between Plasma Erosion Resistance and Surface Roughness

Figure 16 shows relation between plasma erosion rate and delta average surface roughness (ΔR_a), which is estimated from R_a before and after the erosion tests. As the R_a before the erosion test (mirror-polished surface) is different among the specimens, in particular, with bulk having high R_a due to large pits, ΔR_a has been selected to investigate the relation between plasma erosion rate and change in surface morphology.

It seems the specimen with lower erosion rate results in lower ΔR_a , and conventional coating (c-SG) has quite inferior properties. Axial suspension plasma spray with fine powder is found to be quite effective in terms of producing the coatings with high erosion resistance as well as retention of smooth original mirror-polished surface. Among the coatings, the f1-Ax-N shows the best properties, where erosion resistance is 30% better than the conventional coating, and roughness of eroded surface is almost comparable to bulk. Although the plasma erosion resistance is lower, both f5-Ax and f5s-Ax-Ar coatings show lower ΔR_a . Compared with the f1-Ax-Ar and f1-Ax-N, ΔR_a is quite different, meaning that plasma spray conditions also strongly affect the coating properties.

3.8 Inhomogeneity of the Suspension Coatings

As shown in the Fig. 4, speckles are formed in the suspension coatings, which cause imperfectness of the suspension coatings. Figure 17 shows cross-sectional optical micrographs of the suspension coating of f1s-Ax-N, which shows the best properties in this study. Although uniform structure can be seen in Fig. 17(a), defective microstructure is also included in the same coating as shown in Fig. 17(b). The density of the defective speckles with inverted cone shape in the f1s-Ax-N is lower (~about 1/4) than that of f5s-Ax-Ar and f1s-Ax-Ar. It is also found

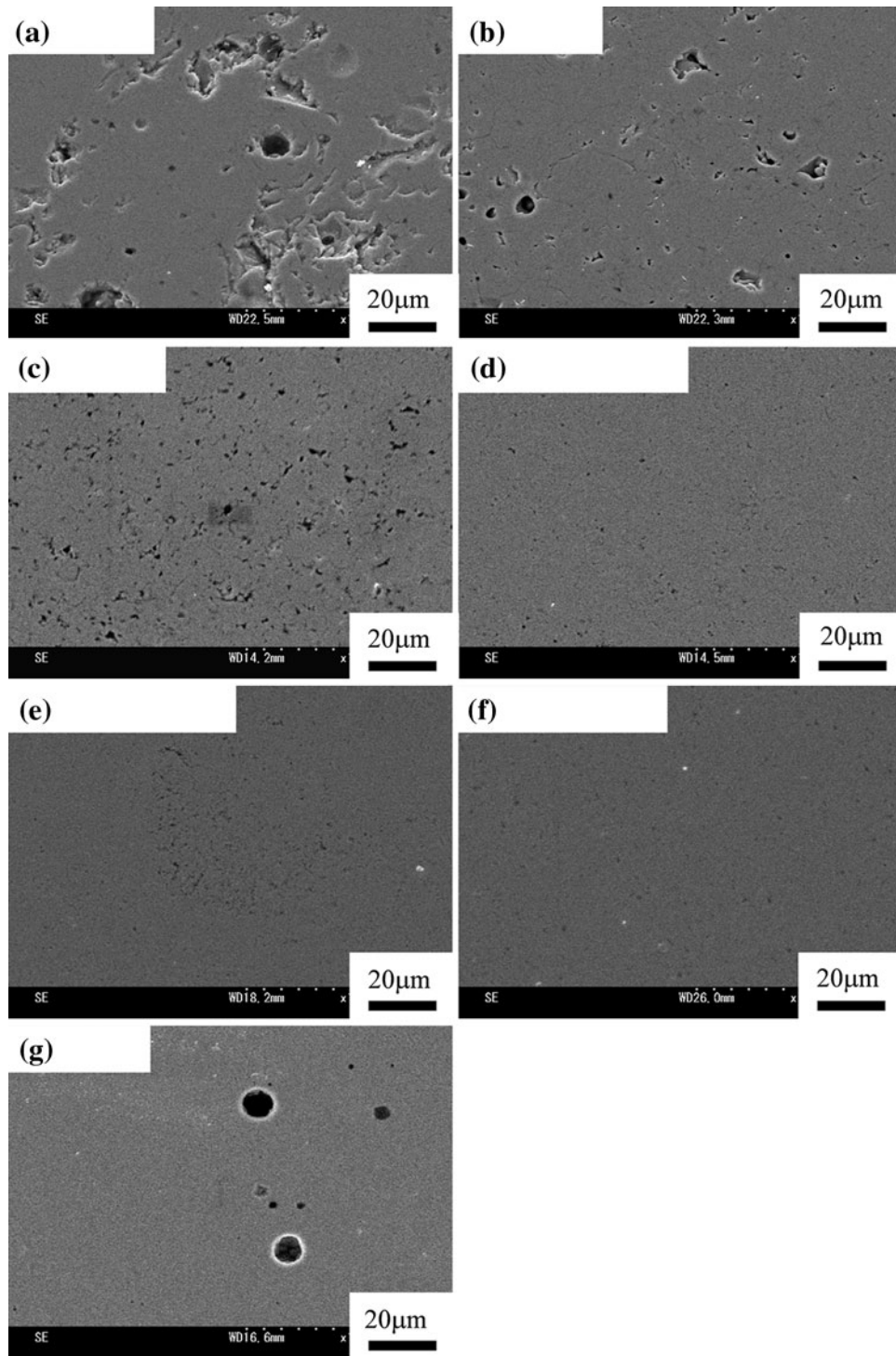


Fig. 13 SEM images of the mirror-polished surfaces before the plasma erosion test. (a) c-SG, (b) c-Ax, (c) f5-Ax, (d) f5s-Ax-Ar, (e) fls-Ax-Ar, (f) fls-Ax-N, and (g) bulk

that no speckles are included in the f5-Ax, c-Ax, and c-SG coatings. This means the speckles are easily generated by the suspension plasma spray process. Here, it should be noted that only uniform region has been selected in this study for evaluation of coating hardness and porosity as mentioned previously.

SEM images of the defects as observed from cross-sectional and top views are shown in Fig. 18. The inverted cone defect has porous structure than surrounding uniform region. In particular, many pores as well as cracks are observed at the boundary, whose structure is similar to that of previous study on HVOF cermet coatings (Ref 32).

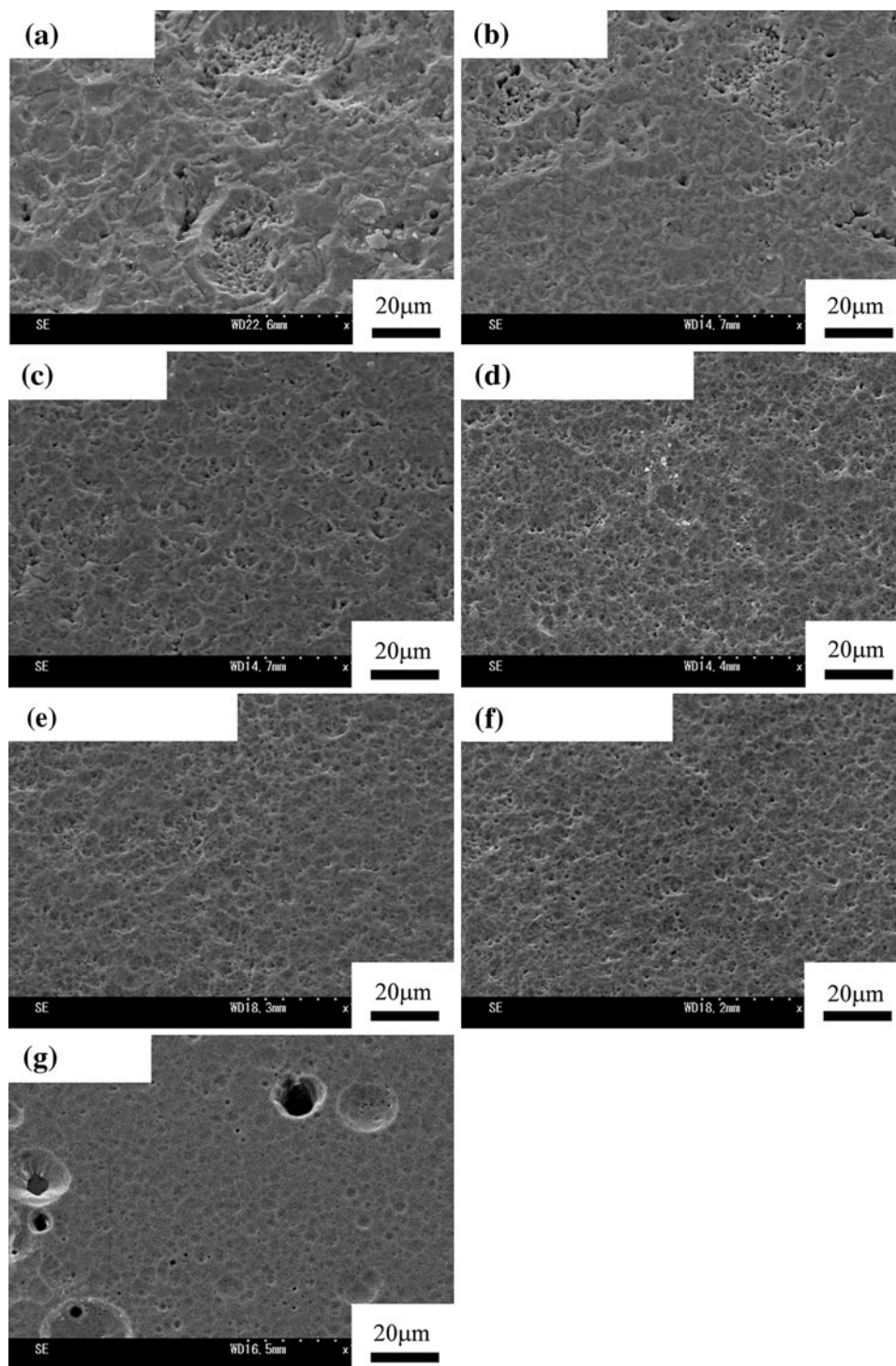


Fig. 14 SEM images of surfaces after the plasma erosion test. (a) c-SG, (b) c-Ax, (c) f5-Ax, (d) f5s-Ax-Ar, (e) fls-Ax-Ar, (f) fls-Ax-N, and (g) bulk

Adversely, dense structure is also formed near the coating surface in the defect. Splats and fine spherical shaped deposits are observed from the defect surface as shown in Fig. 18(b), microstructure of which seems to be similar to that of the uniform region.

Understanding of formation mechanism of the defect is important to improve the coating properties by optimization of suspension plasma spray parameters, such as powder size, powder dispersion in the suspension, selection of solvent, atomization of suspension, suspension

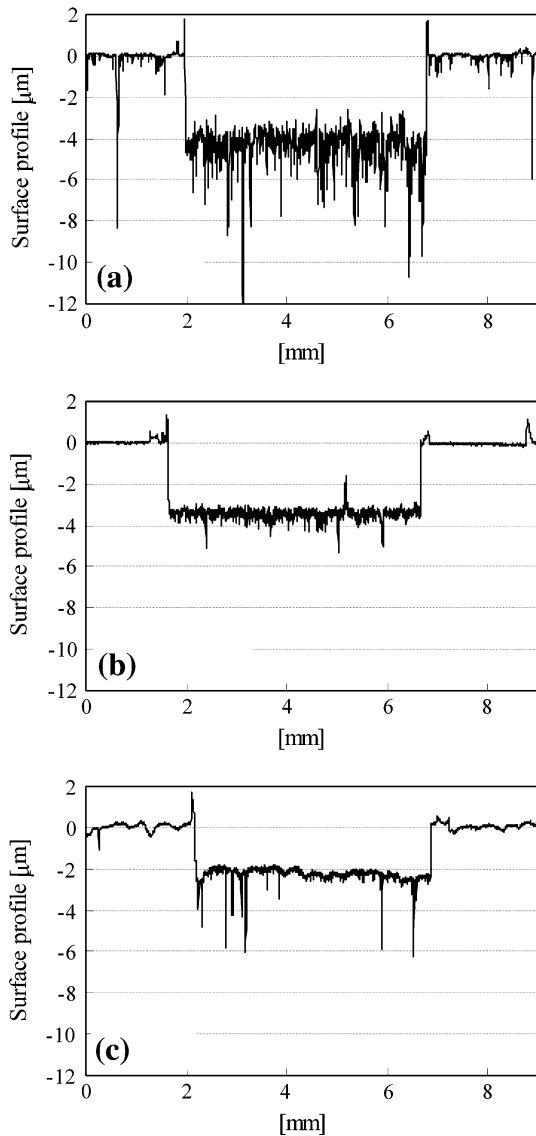


Fig. 15 Surface profiles of eroded (center) and masked (both ends) areas after the plasma erosion test. (a) c-SG, (b) fls-Ax-N, and (c) bulk

feeding rate, plasma power, plasma gas composition, plasma gas feeding rate, stand-off distance, preparation of substrate, and so on. Therefore, investigation at intermediate coating thickness (5, 10, 20, and 50 μm) has been done where effect of substrate roughness has also been studied.

Figure 19 shows R_a of the fls-Ax-N suspension coatings as a function of thickness and effect of substrate roughness. The R_a values and these deviations are obtained by averaging from 5 randomly selected scans. It is clear that R_a on smooth surface becomes higher with increasing thickness as shown in Fig. 19(a). Although 50- μm thickness is formed, no speckles have been observed, and thus, low deviation of roughness of 0.018 μm in R_a and 0.527 μm in R_y is preserved. In the

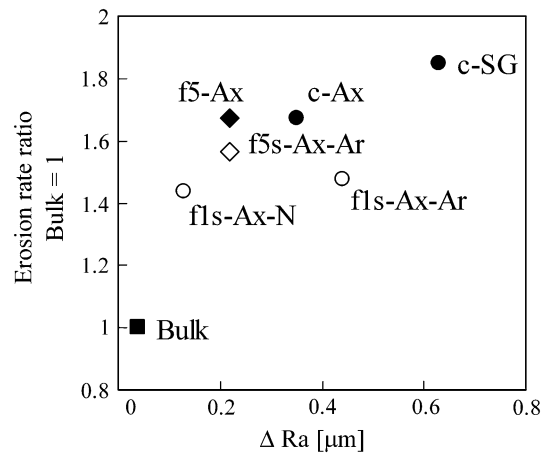


Fig. 16 Relation between plasma erosion rate and delta average surface roughness (ΔR_a)

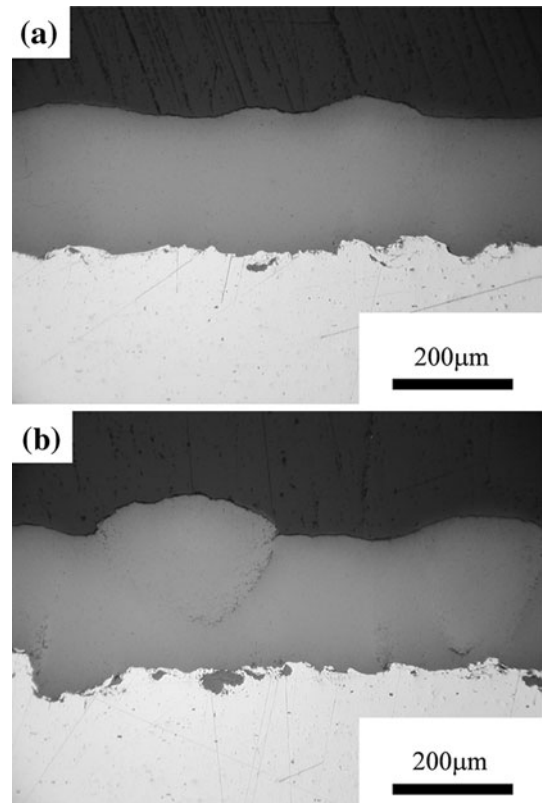


Fig. 17 Cross-sectional optical micrographs of the fls-Ax-N coating with (a) uniform structure and (b) microstructural defects

case of rough substrates in Fig. 19(b), coating roughness is almost comparable to initial substrate roughness up to 20 μm . Also when forming 50 μm , roughness and its deviation are slightly and remarkably higher, respectively. Speckles are clearly generated, being supported from the high deviation of roughness of 0.696 μm in R_a and 17.162 μm in R_y .

The above result clearly indicates that substrate roughness strongly affects speckle formation. Racek (Ref 32) has described that speckles are preferentially grown because of deposition of splashed particles from surrounding area. Therefore, it can be assumed that the projected area produced by sand blasting acts as starting point of the speckle. Although substrate roughness strongly affects speckle formation, speckle density can be decreased with optimization of suspension plasma spray parameters, such as increased plasma enthalpy due to f1s-Ax-Ar and f1s-Ax-N. Further studies are warranted to enable us understand better the mechanism and improve coating uniformity.

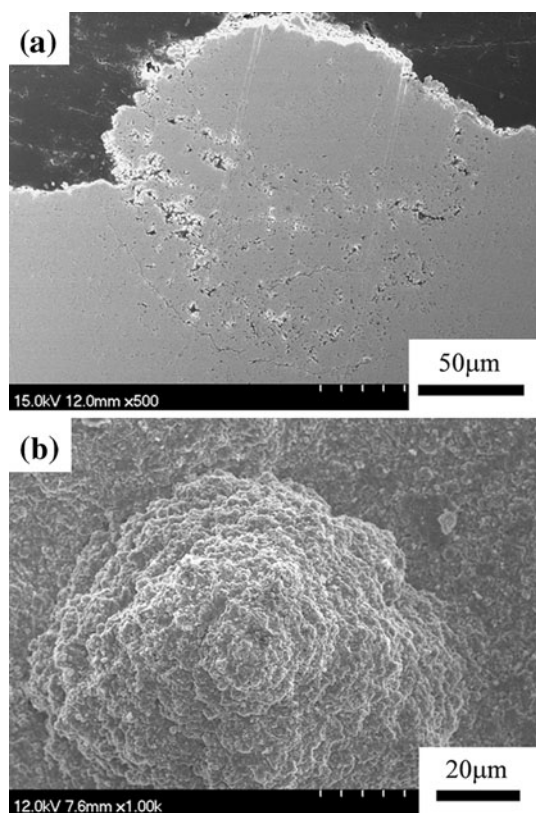


Fig. 18 SEM images of the defects as observed from (a) cross-sectional and (b) top views

4. Conclusions

Yttrium oxide (Y_2O_3) coatings prepared by axial suspension plasma spraying have shown high density, uniform structure, high hardness, high plasma erosion resistance, and retention of smoother surface after plasma erosion. Evaluation results in this study are summarized in Table 6. These will form the basis for a strong

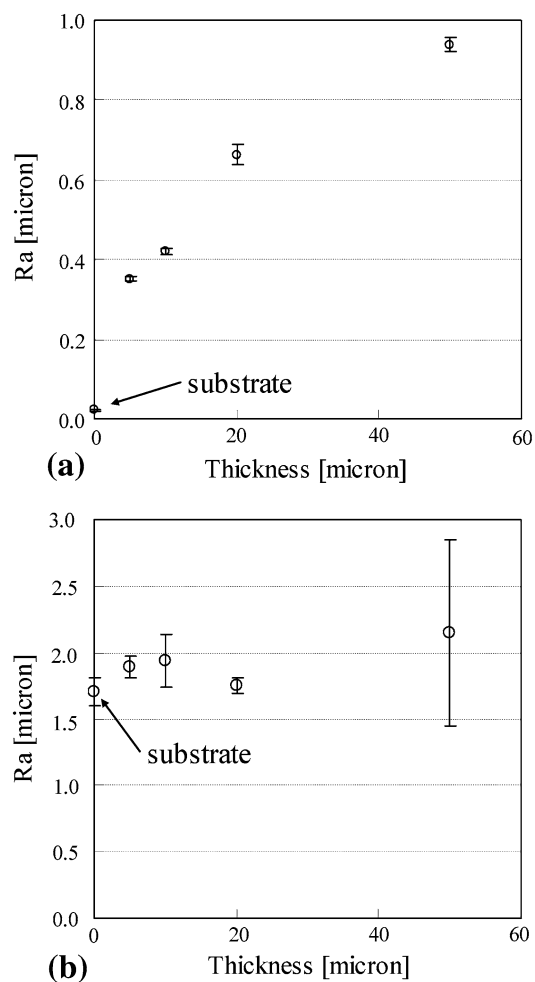


Fig. 19 R_a of the f1s-Ax-N suspension coatings as a function of thickness and effect of substrate roughness

Table 6 Summary of the evaluations in this study

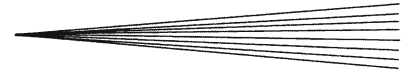
Specimen	Porosity, %	HV	Phase C: cubic M: monoclinic	Plasma erosion resistance Bulk = 1	Eroded surface roughness $\Delta R_a, \mu\text{m}$	Speckles density
c-SG	4.2	390	C	1.86	0.63	Low
c-Ax	4.6	580	$C \gg M$	1.69	0.35	Low
f5-Ax	3.2	430	$C > M$	1.67	0.22	Low
f5s-Ax-Ar	0.4	590	$C \sim M$	1.58	0.22	High
f1s-Ax-Ar	0.3	640	$M > C$	1.50	0.44	High
f1s-Ax-N	0.4	620	$M \gg C$	1.44	0.13	Middle
Y-bulk	<0.1	710	C	1	0.04	...

merit to avoid generation of large-sized particle that easily causes decreased yield ratios of the Si and FPD devices. Fine powder of 1 μm is effective in terms of producing better quality coatings compared with coarser one of 5 μm . Although the properties of the best suspension coating is still inferior to bulk Y_2O_3 for the properties, it is much better than that of the conventional plasma spray coatings. Reduction in the number of inverted cone-shaped defects is one of the key issues, which needs to be addressed in future studies aiming to improve the coating properties.

No lamellar microstructures have been seen from FE-SEM observation in the suspension coatings, which is quite different from the coatings by dry feeding method. Meta-stable phase of monoclinic phase has been formed when using finer powder of less than 5 μm . In particular, use of 1 μm by suspension is effective for producing monoclinic phase, which suggests intense quenching during spraying.

References

- J.W. Coburn and H.F. Winters, Plasma Etching—A Discussion of Mechanisms, *J. Vac. Sci. Technol.*, 1979, **16**(2), p 391-403
- Status and Perspective of Thermal Spray Markets 2004*, Digital Research Institute Inc., Nagoya, Japan, 2004, p 20-33 (in Japanese)
- Y. Kobayashi, Current Status and Needs in the Future of Ceramics Used for Semiconductor Production Equipment, *Proc. 37th Seminar on High-Temperature Ceramics*, K. Matsuhiro, Ed., July 19, 2005 (Osaka, Japan), Japan Ceramics Society, 2005, p 1-7 (in Japanese)
- M. Fukumoto, The Current Status of Thermal Spray in Asia, *J. Therm. Spray Technol.*, 2008, **17**(1), p 5-13
- R. Ohtsuki, Treatment System and Corrosion Resistant Member Used Therefore, Publication of Japanese Patent Application, 2001-226773, 21 August 2001
- J. Kitamura, H. Mizuno, N. Kato, and I. Aoki, Ceramic Coatings Prepared by Plasma Spraying for Semiconductor Production Equipments, *Mater. Trans.*, 2006, **47**(7), p 1677-1683
- J. Kitamura, H. Mizuno, H. Ibe, and I. Aoki, Erosion Properties of Plasma Sprayed Ceramic Coatings Against Process Plasma in Semiconductor Production Equipment, *Thermal Spray 2007: Global Coating Solutions*, May 14-16, 2007 (Beijing, China), ASM International, 2007, p 943-947
- J. Kitamura, H. Ibe, F. Yuasa, and H. Mizuno, Plasma Sprayed Coatings of High-Purity Ceramics for Semiconductor and Flat-Panel-Display Production Equipment, *J. Therm. Spray Technol.*, 2008, **17**(5-6), p 878-886
- T. Morishita, S. Osawa, and T. Itsukaichi, HVOF Ceramic Coatings, *Thermal Spray 2004: Advances in Technology and Application*, May 10-12, 2004 (Osaka, Japan), ASM International, 2004, CD-ROM
- Z. Tang, I. Yaroslavski, P. Hartell, N. Bogdanovic, and A. Burgess, Axial Injection Plasma Spraying Using Micro and Nanopowder Slurries, *Thermal Spray 2008: Crossing Borders*, E. Lugscheider, Ed., June 2-4, 2008 (Maastricht, The Netherlands), DVS, 2008, CD-ROM
- E. Bouyer, F. Gitzhofer, and M.I. Boulos, Suspension Plasma Spraying for Hydroxyapatite Powder Preparation by R.F. Plasma, *IEEE Trans. Plasma Sci.*, 1997, **25**(5), p 1066-1072
- F. Gitzhofer, E. Bouyer, and M.I. Boulos, Suspension Plasma Spraying, U.S. Patent 5,609,921, 3 November 1997
- P. Fauchais, R. Etchart-Salas, V. Rat, J.F. Coudert, N. Caron, and K. Wittmann-T  n  ze, Parameters Controlling Liquid Plasma Spraying: Solutions, Sols, or Suspensions, *J. Therm. Spray Technol.*, 2008, **17**(1), p 31-59
- P. Fauchais and G. Montavon, Latest Developments in Suspension and Liquid Precursor Thermal Spraying, *J. Therm. Spray Technol.*, 2009, **19**(1-2), p 226-239
- B.G. Ravi, S. Sampath, R. Gambino, P.S. Devi, and J.B. Parise, Plasma Spray Synthesis from Precursors: Progress, Issues and Considerations, *J. Therm. Spray Technol.*, 2006, **15**(4), p 701-707
- I. Burlacov, J. Jirkovsky, M. M  ller, and R.B. Heimann, Induction Plasma Sprayed Photo Catalytically Active Titania Coatings and their Characterization by Micro-Raman Spectroscopy, *Surf. Coat. Technol.*, 2001, **113**(1-3), p 456-462
- L. Jua and F. Gitzhofer, Induction Plasma Synthesis of Nano-Structured SOFCs Electrolyte Using Solution and Suspension Plasma Spraying: A Comparative Study, *J. Therm. Spray Technol.*, 2010, **19**(3), p 566-574
- P. Fauchais, V. Rat, C. Delbos, J.F. Coudert, T. Chartier, and L. Bianchi, Understanding of Suspension dc Plasma Spraying of Finely Structured Coating for SOFC, *IEEE Trans. Plasma Sci.*, 2005, **33**(2), p 920-930
- P. Fauchais, R. Etchart-Salas, C. Delbos, M. Tognovi, V. Rat, J.F. Coudert, and T. Chartier, Suspension and Solution Plasma Spraying of Finely Structured Coatings, *J. Phys. D Appl. Phys.*, 2007, **40**, p 2394-2406
- F.L. Toma, G. Bertrand, D. Klein, C. Coddet, and C. Meunier, Nanostructured Photocatalytic Titania Coatings Formed by Suspension Plasma Spraying, *J. Therm. Spray Technol.*, 2006, **15**(4), p 587-592
- O. Tingaud, A. Bacciochini, G. Montavon, A. Denoirjean, and P. Fauchais, Suspension dc Plasma Spraying of Thick Finely-Structured Ceramic Coatings: Process Manufacturing Mechanism, *Surf. Coat. Technol.*, 2009, **203**(15), p 2157-2161
- J. Karthikeyan, C.C. Berndt, J. Tikkanen, S. Reddy, and H. Herman, Plasma Spray Synthesis of Nanomaterial Powders and Deposits, *Surf. Coat. Technol.*, 1997, **238**(2), p 275-286
- R. Rampon, F.L. Toma, G. Bertrand, and C. Coddet, Liquid Plasma Sprayed Coatings of Yttria-Stabilized Zirconia for SOFC Electrolytes, *J. Therm. Spray Technol.*, 2006, **15**(4), p 682-688
- R. Rampon, C. Filiatre, and G. Bertrand, Suspension Plasma Spraying of YPSZ Coatings: Suspension Atomization and Injection, *J. Therm. Spray Technol.*, 2008, **17**(1), p 105-114
- H. Kassner, R. Siegert, D. Hathiramani, R. Vassen, and D. Stoeber, Application of Suspension Plasma Spraying (SPS) for Manufacture of Ceramic Coatings, *J. Therm. Spray Technol.*, 2008, **17**(1), p 115-123
- J. Oberste Berghaus, B. Marple, and C. Moreau, Suspension Spraying of Nanostructured WC-12Co Coatings, *J. Therm. Spray Technol.*, 2006, **15**(4), p 676-681
- S. Bouaricha, J. Oberste-Berghaus, J.-G. Legoux, C. Moreau, and D. Ghosh, Production of Samarium Doped-Ceria Plasma Sprayed Nano-Coatings Using an Internal Injection of a Suspension Containing Nanoparticles, *Thermal Spray 2005: Explore Its Surfacing Potential*, E. Lugscheider, Ed., May 2-4, 2005 (Basel, Switzerland), DVS, 2005, CD-ROM
- J. Oberste-Berghaus, S. Bouaricha, J.-G. Legoux, C. Moreau, and T. Chraska, *Thermal Spray 2005: Explore Its Surfacing Potential*, E. Lugscheider, Ed., May 2-4, 2005 (Basel, Switzerland), DVS, 2005, CD-ROM
- J.O. Berghaus, S. Bouaricha, J.-G. Legoux, and C. Moreau, Suspension Plasma Spraying of Nano-Ceramics Using an Axial Injection Torch, *Thermal Spray 2005: Explore Its Surfacing Potential*, E. Lugscheider, Ed., May 2-4, 2005 (Basel, Switzerland), DVS, 2005, CD-ROM
- D. Waldbillig, O. Kesler, Z. Tang, and A. Burgess, Suspension Plasma Spraying of Solid Oxide Fuel Cell Electrolytes, *Thermal Spray 2007: Global Coating Solutions*, May 14-16, 2007 (Beijing, China), ASM International, 2007, p 677-682
- J. Kitamura, H. Ibe, F. Yuasa, Z. Tang, and A. Burgess, Structural, Mechanical and Erosion Properties of Plasma Sprayed Yttrium Oxide Coatings by Axial Injection of Fine Powder Slurries for Semiconductor and Flat-Panel-Display Applications, *Thermal Spray 2009: Expanding Thermal Spray Performance to*



- New Markets and Applications*, May 4-7, 2009 (Las Vegas, NV, USA), ASM International, 2009, p 567-572
32. O. Racek, The Effect of HVOF Particle-Substrate Interactions on Local Variations in the Coating Microstructure and the Corrosion Resistance, *J. Therm. Spray Technol.*, 2010, **19**(5), p 841-851
 33. H. Ibe, K. Sato, F. Yuasa, H. Mizuno, and J. Kitamura, Influence of Powder Properties and Plasma Spray Conditions on Erosion Resistance of Yttrium Oxide Coatings against Halogen Plasma for Dry Etching Process in Semiconductor and Electronic Applications, *Thermal Spray 2009: Expanding Thermal Spray Performance to New Markets and Applications*, May 4-7, 2009 (Las Vegas, NV, USA), ASM International, 2009, p 541-546
 34. K. Hirata, K. Moriya, and Y. Waseda, High Temperature Thermal Expansion of ThO_2 , MgO and Y_2O_3 by X-Ray Diffraction, *J. Mater. Sci.*, 1977, **12**(4), p 838-839
 35. G.J. Vogt, Synthesis of the Monoclinic Yttria by Thermal Plasma Processing, *Proc. Symposium on High Temp. Mater. Chem. 4th*, 1988, p 572-583
 36. T. Atou, K. Kusaba, K. Fukuoka, M. Kikuchi, and Y. Syono, Shock-Induced Phase Transition of Mn_2O_3 (M = Sc, Y, Sm, Gd, and In)-Type Compounds, *J. Solid State Chem.*, 1990, **89**, p 378-384